Research Article

Chemical Review and Letters
journal homepage: www.chemrevlett.com
ISSN (online): 2645-4947 (print) 2676-7279

Application of response surface methodology for modeling and optimization of basic yellow 28 decolorization using sonoelectrochemistry

Masoud Rohani Moghadam[1,*], Saeideh Pirozi[1], Fariba Beigmoradi[1], Alireza Bazmandegan-Shamili[1], Hamidreza Masoodi[1]

[1]*Department of Chemistry, Faculty of Science, Vali-e-Asr University, Rafsanjan 77188-97111, Iran*

ARTICLE INFO

Article history:
Received 17 January 2023
Received in revised form 2 February 2023
Accepted 22 February 2023
Available online 2 April 2023

Keywords:
Sonoelectrochemistry
Decolorization
Basic Yellow 28
Desirability Function
Central composite design

ABSTRACT

In this context, a rapid sonoelectrochemical decolorization of aqueous Basic Yellow 28 (BY 28) solutions on a batch reactor using an ultrasound probe (20 kHz) combined with a rectifier was studied. The residual dye was determined by UV-Vis spectrophotometric technique (λ=440 nm). A 2^5 central composite design (CCD; half-fraction) has been chosen to elucidate the combined effect of five process variables; applied potential, ultrasonic power, pH, electrolyte concentration and temperature. The decolorization percentage (a measure of remediation) and the energy efficiency (a measure of energy saving) were considered responses that were optimized simultaneously using the desirability function. Under the optimum conditions of applied potential (11.15V), ultrasonic power (592.7 W), pH (5), KCl concentration (0.08 mol L^{-1}) and temperature (20.8°C), 99.99% decolorization percent and 0.83 mmol$kW^{-1}h^{-1}$ energy efficiency was predicted, that was close to obtained experimental results (97.5± 1.1% and 0.75±0.06 mmolkWh^{-1}). The degradation products formed were studied using UV-Vis and HPLC-UV after sonoelectrochemical degradation.

1. Introduction

Dyes and pigments are organic or inorganic chemicals extensively used in various industrial branches such as dye manufacturing, textile, leather, paper, food, cosmetics and carpet. Due to large-scale production and wide application, synthetic dyes can cause significant environmental pollution and critical health hazards. The industrial effluent containing unused colored materials discharged into water sources creates severe pollution problems by releasing toxic and potentially carcinogenic substances into the environment. Furthermore, even small amounts of dyes lead to colored wastewater that reduces sunlight penetration and thus hinders the process of photosynthesis. Therefore, the decolorization of industrial wastewater prior to disposal into receiving water bodies is required [1]. Organic dyes are classified into reactive, direct, acid, basic, mordant, disperse, solvent, vat and basic dyes. Basic Yellow 28 (BY 28), as a basic dye, is a water-soluble dye widely used for dyeing nylon, polyesters and polyacrylonitrile [2] and is, therefore, one of the most common pollutants in the textile industry. Various technologies for the decolorization of BY 28 involve the search for innovative materials and effective methods such as liquid-liquid extraction [1], adsorption [2-8], phothocatalytical [9, 10], photoelectron-fenton [11], nanoscale zero-valent iron [12] and electrochemical [13-17] techniques. However, long remediation time [1-9], small sample volume [2, 9, 10, 12, 14, 17], secondary pollution[1-3, 5] and expensive materials [11, 15-17] hindered the possible scale-up and industrial application.

Electrochemistry, a simple, eco-friendly and effective method that applies a potential capable of either oxidizing or reducing the interest substrate, have been widely applied in the decolorization process. Different electrochemical methods have been used for this purpose, including direct oxidation/reduction, electrocoagulation and indirect oxidation [14, 15, 18, 19]. Indirect oxidation is more favorable due to the faster reaction rate than the two other methods, based on the homogeneous reaction between electrochemically generated oxidizing species and dyes. Recently, a combination of electrochemistry with other technologies has been used to enhance treatment performance [20-22]. Sonoelectrochemistry is an attractive hybrid technology in which electrochemical and ultrasound processes are combined. Diffusion of

* Corresponding author.; e-mail: m.rohani@vru.ac.ir
https://doi.org/10.22034/crl.2023.381956.1197

ultrasound waves within a liquid (acoustic cavitations) produces small local sites with high pressure and temperature in a short period, generating radical species that are appropriate for destroying organic compounds. Instead, ultrasonic waves increase the mass transfer rate in an aqueous solution via increasing turbulence [23].

This study aims to develop a rapid treatment technique for color degradation with consideration of a possible industrial application. To achieve this goal, the ability of sonoelectrochemical decolorization of BY 28 within one minute, using persistent electrodes (stainless steel) in relatively larger sample volumes (600 ml), was examined. Influential categorical factors, including electrolyte type, electrode material and electrode size, were studied using the one-factor at a time (OFAT) manner. Furthermore, critical numerical factors, including ultrasonic power, applied potential, initial pH, electrolyte concentration and temperature, were investigated and optimized using central composite design (CCD; half fractional) and desirability function to obtain maximum decolorization with a minimum of energy consumption. UV-Vis absorbance spectra (200-700 nm) at several reaction times were collected to study the decolorization process. Also, a sonoelectrochemical decolorized solution was analyzed by HPLC-UV and compared with an untreated sample.

2. Experimantal

2.1. Chemicals

Textile dye, BY 28 (MW: 433 g mol^{-1}), was purchased from Rifazol (commercial name Bezacryl Goldgelb GL 200) and used without further purification. The structure of BY 28 is shown in Schem.1. A dye solution was prepared by dissolving the dye in distilled water. All the other chemicals were of analytical grade and were obtained from Merck Company (Germany).

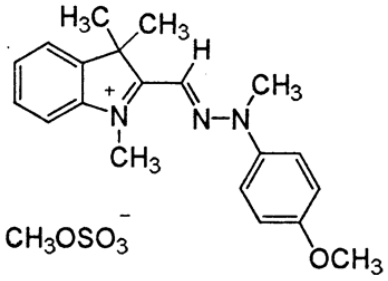

Scheme 1. Chemical structure of BY28.

2.2. Experimental setup

Experimental runs were generated and evaluated using Design-Expert software (V. 8.0.2 trail; Stat-Ease Inc., Minneapolis, Minnesota). A schematic diagram of the sonoelectrochemical process is shown in Fig.1.

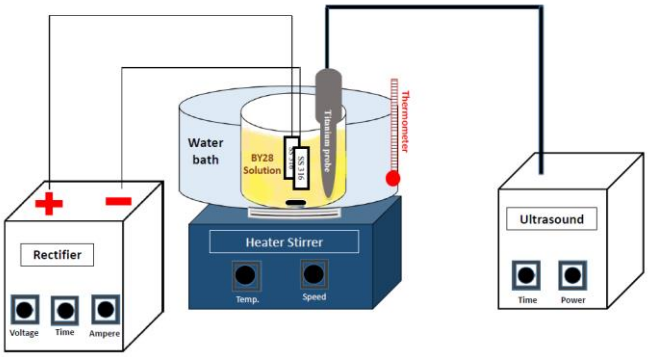

Figure 1. The schematic diagram of the used sonoelectrochemical apparatus.

The electrochemical part was composed of a rectifier with DC-Output (Pulse 440 Timer Controlled Rectifier, Nanoabkar-Isatic, Iran). Two stainless steel electrodes (SS 316) with 41.8 cm^2 surface area were positioned vertically in the middle of a glass reactor with an inner gap of 5 cm. The reactor was placed in a water bath, and the solution temperature was manually controlled. The solution temperature was measured with a digital thermometer fixed on the reactor's inner wall. FS-600 Ultrasonic Processing (China) with a titanium probe (11 mm) was applied that produced 20 kHz frequency with tunable power up to 600 W.

2.3. Analytical instrument

The pH of samples was measured by pH meter (Genway, 8602, UK) and adjusted by adding NaOH or H_2SO_4 solutions(1 N).The decolorization process was investigated by an HPLC-UV (Sykam, Germany) with a reverse phase C_8 column (250 mm × 4.6 mm i.d., 5 µm. Dye concentration was determined at 440 nm by a double-beam UV/Vis spectrophotometer (PG instrument, UK) according to a calibration curve. The percentage of decolorization was calculated according to the fallowing equation.

$$PD = \frac{C_i - C_f}{C_i} \times 100 \quad (1)$$

PD is the percentage of decolorization, C_i is the initial concentration ($mmolL^{-1}$) of BY 28, and C_f is its concentration ($mmolL^{-1}$) at a given reaction time. The energy efficiency of the process, defined as the amounts of converted BY 28 divided by consumed electrical energy [24], is calculated based on Eq 2.

$$EE = \frac{(C_i - C_f)V}{E} \quad (2)$$

EE is energy efficiency ($mmolkWh^{-1}$), *V* is the volume of BY 28 solution (L) and *E* as required electrical energy (kWh) is expressed as follows.

$$E = UIt + Qt \quad (3)$$

where, *U* is the applied potential(Volt), and *I* is the average electrical current(Amp.) of rectifier. Q is the ultrasonic power (Watt), and t is the ultrasonic probe's treatment time (hour).

2.4. Experimental design

Central composite design (CCD), as one of the well-known response surface methodology (RSM) [25], has been used to express the relationships between experimental responses and effective parameters. The CCD consists of several factorial, axial and central points. In the present work, 32 experiments were designed according to the half-fractional CCD for five effective factors. Factors levels are shown in Table 1. Percent of decolorization and energy efficiency were considered as the two responses that were simultaneously optimized using Global Desirability Function (*D*). This function consists of two simple components calculated (Eq. 4) for each response individually and named as partial desirability function (d_i). In this way, the multicriteria problem is reduced to a single criterion problem in Global Desirability Function (Eq. 5) [26].
The *D* value of zero or near zero is not acceptable, while a desirable *D* is assigned to a value near one, depending on the closeness of the response to its purposed value. Since a maximum amount of d_i was desirable in this work, the related partial desirability function ($d_{i,max}$) was calculated according to Eq.4.

$$d_{i,max} = \frac{Y_i - Y_{min}}{Y_{max} - Y_{min}} \quad (4)$$

In this equation, Y_i is the experimental response, and Y_{max} and Y_{min} are the maximum and minimum values of experimental responses. As previously mentioned, the individual desirability values are combined as a geometric mean to give *D*, which is defined as:

$$D = (d_{1,max} \times d_{2,max})^{\frac{1}{2}} \quad (5)$$

Although a maximum value of *D* is desirable, the goal of an optimization procedure is to find a set of conditions that will meet all the goals, but not necessarily to get a *D* value equal to one [27, 28]. However, optimum values of the investigated factors were determined by solving the regression equation and according to related response surface plots.

3. Results and discussion

3.1. Selection of electrolyte type

The supporting electrolytes are one of the most critical factors that affect the sonoelectrochemical decolorization process. So, the effect of different salts including NaCl, KCl, Na_2SO_4 and Na_2CO_3 on the responses was investigated, while their concentration was adjusted to 0.06 $molL^{-1}$. Under the exact condition of applied potential (12.5 V), temperature (25°C), ultrasonic power (360 W) and pH (7.0), the impact of electrolyte type is demonstrated in Fig.2. As is shown, the decolorization percentages and energy efficiencies were significantly better when NaCl and KCl were used as electrolyte. This is likely due to the generation of OCl^- which has sufficient oxidation potential for distortion of BY 28. Indeed,since relatively better results was achieved using KCl compare to NaCl, it was selected as the supporting electrolyte for further experiments.

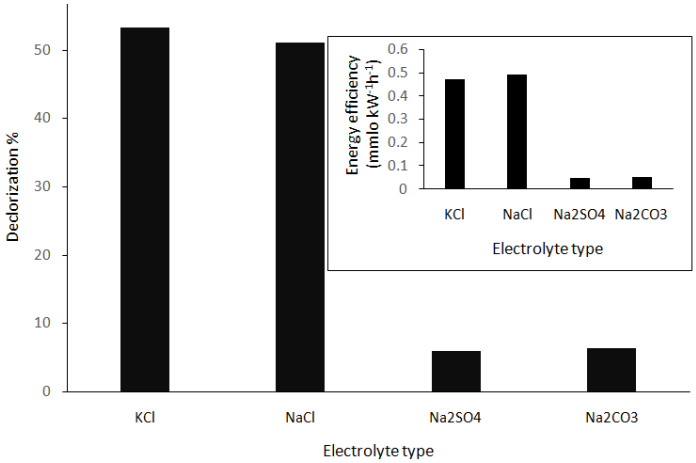

Figure 2. The effect of different electrolytes on the decolorization percentage and energy efficiency in the BY 28 sonoelectrochemical decolorization.

3.2. Selection of type and size of electrodes

The type and size of electrodes were other parameters that affected the sonoelectrochemical decolorization of BY 28. Aluminum (Al 99.5) and stainless steel electrodes (SS 316) with flat and tube shapes with the same surface area (~42 cm^2) were investigated. According to obtained results, 95% and 7% decolorization was achieved using SS316and Al 99.5, respectively. Furthermore, the influence of electrode shape was not considerable. Afterwards, size effect was investigated using rectangular SS316 electrodes with 41.8, 8.2, and 2.4cm^2 surface areas. Based on experimental results, the best decolorization and energy efficiency were obtained when 41.8cm^2 electrodes were used.

3.3. Optimization of numerical factors

According to initial investigations, pH, applied potential, ultrasonic power, electrolyte concentration, and temperature were critical numerical factors that must be optimized to achieve maximum decolorization with minimum energy consumption. For this purpose, Design Expert software designed a half-fractional CCD consisting of 16 factorial points, 10 axial points, and 6 central points. The design matrix with predicted and actual responses is shown in Table 1.

3.4. Mathematical model equation using CCD

Different mathematical models were constructed, and variance analysis was used to compare models and achieve the best one for each response. This study's experimental results were fitted in quadratic and cubic equations for decolorization percentage and energy efficiency, respectively. The final equations in terms of actual factor levels are given below:

Table 1. Factors levels and design matrix with actual and predicted values of *PD* and *EE*.

Factor	Level + α	+1	0	-1	- α	(α=2)
Potential (V)	20	16.25	12.50	8.75	5	
USP (W)	600	480	360	240	120	
pH	12.0	9.5	7.0	4.5	2.0	
[KCl] (mol L^{-1})	0.1	0.08	0.06	0.03	0.01	
Temp. (°C)	40	35	30	25	20	

	Factors					Actual responses		Predicted response	
Run #	Potential	USP	pH	Temp.	[KCl]	PD	EE	PD	EE
1	16.25	480	9.5	35	0.08	95.59	0.62	115.57	0.78
2	12.5	360	7	40	0.06	49.74	0.43	35.78	0.58
3	8.75	240	4.5	25	0.08	78.72	1.1	85.13	1.03
4	8.75	240	4.5	35	0.03	28.05	0.4	30.23	0.64
5	12.5	360	12	30	0.06	53.90	0.37	67.87	0.35
6	12.5	120	7	30	0.06	43.18	1.07	56.49	1.05
7	8.75	240	9.5	25	0.03	9.15	0.28	11.08	0.42
8	8.75	240	9.5	35	0.08	13.28	0.21	25.14	0.15
9	12.5	360	7	20	0.06	61.36	0.54	66.60	0.69
10	12.5	360	2	30	0.06	78.89	1.2	80.60	1.18
11	12.5	600	7	30	0.06	84.14	0.45	91.90	0.43
12	16.25	240	9.5	25	0.08	96.5	1.35	91.17	1.32
13	16.25	480	4.5	25	0.08	92.34	0.62	88.23	0.56
14	8.75	480	9.5	35	0.03	39.3	0.29	25.48	0.18
15	8.75	480	4.5	25	0.03	90.16	0.79	85.46	0.68
16	12.5	360	7	30	0.06	75.54	0.25	74.19	0.64
17	16.25	480	9.5	25	0.03	95.99	0.85	91.50	0.98
18	12.5	360	7	30	0.06	67.95	0.79	74.19	0.64
19	20	360	7	30	0.06	96.9	0.85	108.76	0.83
20	16.25	240	4.5	25	0.03	67.57	0.79	64.17	0.79
21	16.25	240	9.5	35	0.03	86.3	0.85	80.51	0.64
22	8.75	480	4.5	35	0.08	56.12	0.79	65.3	0.78
23	5	360	7	30	0.06	24.3	0.04	39.36	0.02
24	12.5	360	7	30	0.06	96.75	0.86	74.19	0.64
25	12.5	360	7	30	0.01	5.28	0.12	19.18	0.10
26	12.5	360	7	30	0.06	97.34	0.87	74.19	0.64
27	12.5	360	7	30	0.06	96.52	0.9	74.19	0.64
28	16.25	240	4.5	35	0.08	29.97	0.13	44.00	0.22
29	12.5	360	7	30	0.1	96.52	0.89	63.90	0.87
30	12.5	360	7	30	0.06	92.34	0.45	74.19	0.64
31	16.25	480	4.5	35	0.03	45.33	0.23	44.34	0.25
32	8.75	480	9.5	25	0.08	25.22	0.11	36.14	0.19

USP: ultrasonic power, PD: percent of decolorization, EE: energy efficiency.

$$PD=+139.54053-(9.63716\times Potential)+(0.07376\times Power)-(53.26050\times pH)+(6.06749\times Temp)+(1887.96208\times [KCl])-(0.23002\times Temp^2)-(13655.37919\times [KCl]^2)+(2.03513\times Potential\times pH)+(0.8846\times pH\times Temp) \quad (6)$$

$$EE=+11.02114-(0.92053\times Potenial)-(0.01386\times Power)-(0.98671\times pH)-(0.27985\times Temp)+(50.88752\times [KCl])+(0.021422\times Potential^2)+(2.34809\times 10^{-5}\times Power^2)+(0.08984\times pH^2)-(870.23320\times [KCl]^2)+(0.027267\times pH\times Potential)+(0.038922\times Potential\times Temp)+(1.55208\times 10^{-4}\times Temp\times Power)+(6.99259\times 10^{-4}\times Potenial^3)+(2.01341\times 10^{-8}\times Power^3)-(4.04000\times 10^{-3}\times pH^3)+(4810.24234\times [KCl]^3)-(1.71556\times 10^{-3}\times Potenial^2\times Temp) \quad (7)$$

3.5. Analysis of variance (ANOVA)

ANOVA is a statistical method that subdivides the total variation of data into parts related to the specific sources of variation to test hypotheses on the model parameters. It is also used to check the significance and fitness of the provided model. The ANOVA tables of the decolorization percentage and energy efficiency are

shown in Tables 2 and 3, respectively. As the tables show, the independent variables and some of their interactions are the significant factors that affect the responses. According to the tables, the *p*-values of the models for *PD* and *EE* were < 0.0001 and 0.0058, respectively. So, it can be concluded that both responses (*PD* and *EE*) fit the models well at a 95% confidence level. Moreover, the lack of fit test is another suitable statistical parameter for checking the model's fitness. It compares the residual error with the pure error using replicated data of the central points. A model with a significant lack of fit value lacks prediction efficiency, while a non-significant lack of fit value in the model is highly desirable. The lack of fit *p*-values of 0.2520 for *PD* and 0.8726 for *EE* implies that the lack of fit is not significant relative to the pure error, which proves the adequacy of the models. Multiple regression analysis of the response is another important test that measures the amount of variation around the mean explained by the model. Based on the experimental and predicted responses, *R*-squared values 0.7904 for *PD* and 0.8302 for *EE* were obtained. "Adequate precision" that expresses a predicted response relative to its associated error is a measure of signal-to-noise ratio. While adequate precision values greater than 4 are enough for suitable navigation of design space, 12.417 and 8.095 was calculated for *PD* and *EE*, respectively.

Table 2. The ANOVA table of decolorization percentage with quadratic model.

Source	Sum of squares	DF	Mean square	F-value	Prob>F	
Model	22577.50	9	2508.61	9.22	< 0.0001	Significant
A	7168.78	1	7168.78	26.35	< 0.0001	
B	1880.27	1	1880.27	6.91	0.0153	
C	246.46	1	246.46	0.91		
D	1425.27	1	1425.27	5.24	0.0321	
D^2	987.65	1	987.65	3.63	0.0699	
E^2	1427.33	1	1427.33	5.25	0.0319	
AC	5824.36	1	5824.36	21.41	0.0001	
CD	1956.51	1	1956.51	7.19	0.0136	
Residual	5985.75	22	272.08			
Lack of Fit	5173.67	17	304.33	1.87	0.2520	Not significant
Pure Error	812.07	5				
Cor Total	28563.24	31				

DF: Degree of freedom, A: Potential, B: Power, C:pH, D: Temp., E: [KCl].

Table 3. The ANOVA table of energy efficiency with cubic model.

Source	Sum of squares	DF	Mean square	F-value	Prob>F	
Model	3.17	17	0.19	4.03	0.0058	significant
A	0.024	1	0.024	0.52	0.4820	
B	2.006×10^{-3}	1	2.006×10^{-3}	0.043	0.8383	
C	0.016	1	0.016	0.35	0.5639	
D	6.050×10^{-3}	1	6.050×10^{-3}	0.13	0.723	
E	5.689×10^{-3}	1	5.689×10^{-3}	0.12	0.7314	
A^2	0.085	1	0.085	1.84	0.1964	
B^2	0.018	1	0.018	0.40	0.5383	
C^2	0.029	1	0.029	0.62	0.4435	
E^2	0.044	1	0.044	0.96	0.3447	
AC	1.05	1	1.05	22.54	0.0003	
AD	0.089	1	0.089	1.91	0.1888	
BD	0.14	1	0.14	2.99	0.1057	
A^3	0.065	1	0.065	1.41	0.2553	
B^3	0.058	1	0.058	1.25	0.2819	
C^3	0.19	1	0.19	4.12	0.0617	
E^3	0.14	1	0.14	3.11	0.0998	
A^2D	0.078	1	0.078	1.67	0.2168	
Residual	0.65	14	0.046			
Lack of Fit	0.28	9	0.031	0.43	0.8726	Not significant
Pure Error	0.37	5	0.073			
Cor Total	3.82	31				

Interaction between some factors in the responses is shown in Fig. 3. Significant interaction is observed between pH and Temp in the *PD* model (Fig. 3.a). At the high pH level, temperature changes have not considerably affected the decolorization, while it increases up to ~ 100% when temperature decreases to 25 °C, at pH=4.5. On the other hand, a maximum PD of around 60% is observed at pH=9.5 for a warmer solution, while acidic media is desirable in a more cooled solution that reaches to ~ 100% at pH=4.5. Another significant interaction is observed between pH and potential (Fig. 3.b). In alkali conditions, potential and *PD* have a direct relationship, and complete decolorization of BY 28 is achieved with potential values greater than 15 V. In contrast, at low pH levels, the effect of potential on *PD* is negligible. On the other side, when the potential is equal to 8.8 V, an acidic solution is desirable. However when high potential values are applied, a maximum DP of ~100% appears in an alkali media. As it appears in Fig.3.c, the interaction between [KCl] and US power is not important in the model, and higher values of both factors are desirable.

Although complete decolorization of BY 28 was the goal of this work, we aimed to perform it with minimum energy consumption. In other words, we searched conditions that thoroughly the decolorization happens with maximum energy efficiency. As shown in Fig. 3.d, the temperature effect is not essential at a low potential level. However, at a high potential level, better results are obtained when the solution temperature is set at 25 °C. In the case of potential effect, it is seen that the response increases with an increase in applied potential at 25 °C, while at the high level of temperature, *EE* reaches a maximum when potential is close to 12.5 V. The applied potential also interacts with the pH (Fig. 3.e). In acidic media, EE decreases with an increase in the potential; conversely, the state occurs in alkali conditions. The same situation can be observed with the pH effect. Another interaction between temperature and US power (Fig. 3.f), where an increase in *EE* is viewable when low US power is applied, and vice versa. A similar effect can be seen on the US power.

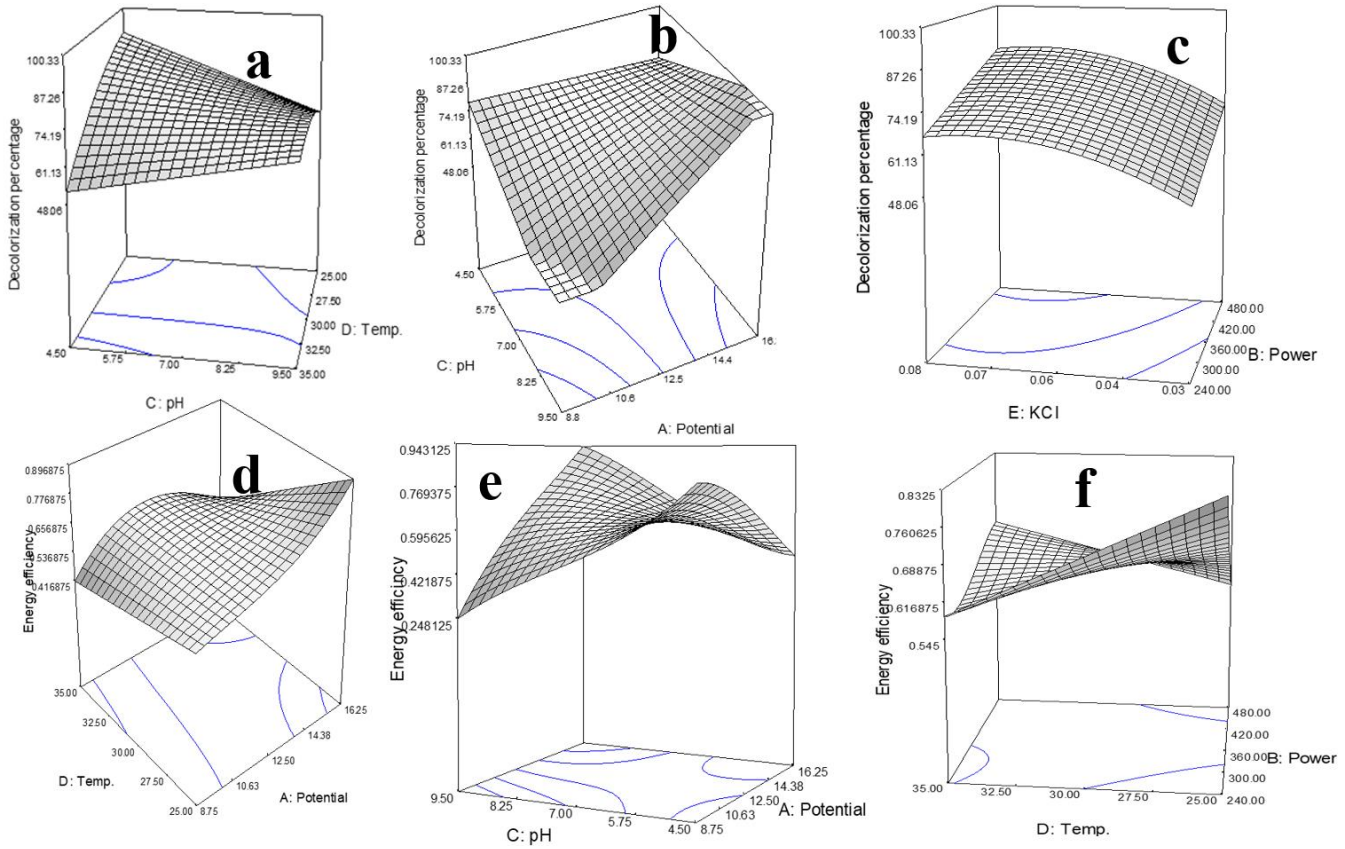

Figure 3. The response surface plots of the percent of decolorization as a function of (a) pH and temperature (°C), (b) pH and potential (V), (c) [KCl] (molL^{-1}) and ultrasonic power (W), as well as the response surface plots of the energy efficiency as a function of (d) potential (V) and temperature (°C), (e) pH and potential (V) and (f) temperature (°C) and ultrasonic power.

3.6. Optimization using Desirability Function

After studying the effects of the factors on each response, the factors were simultaneously optimized for both of the responses by using the desirability function. Responses were transformed into individual desirability scales of d_1 and d_2 for *PD* and *EE*, respectively. Consequently, the global desirability value was determined as the geometric mean of the individual desirability functions by a feasibility grid search over the domain by the software. The optimized formulation was

achieved at potential=11.15V, ultrasonic power=592.7W, pH=5, temperature=20.8˚C and [KCl]=0.08mol L^{-1} with 0.996 desirability value (*D*) that predicted 99.99% and 0.83 mmolkWh^{-1} for DP and EE, respectively. In order to model validation, 4 batches under conditions as close as possible to the optimum values were examined. In applied conditions of potential=11.3±0.2 V, ultrasonic power=591±4 W, pH=5.0±0.1, temperature=21±1˚C and [KCl]=0.08 molL^{-1}, experimental responses of 97.5± 1.1% and 0.75±0.06 mmolkWh^{-1} was achieved for *PD* and *EE*, respectively (with four replication). The closeness of the actual and predicted responses proves the excellent ability of the constructed models.

3.7. Durability of the electrodes

If a large scaled wastewater treatment plant is desired, repair and maintenance should be considered. The shelf life of the electrodes is an essential issue in the present work because, with more stable electrodes, less maintenance cost is required. In order to study the stability of the electrode, its weight loss was determined after more than 500 tests in very different conditions and even a few textile dyes (such as Acid Blue 25 and Disperse Red 60). It was found that only 0.3% weight loss occurred, which was seen in the form of small black spots on the electrode's surface. So, it can be concluded that the used electrodes can remain without significant destruction for a long time.

3.8. UV–Vis spectra analysis

The variation of absorbance spectra of BY 28 during the sonoelectrochemical reaction is shown in Fig. 4. The UV-Vis spectra of BY 28 solutions were characterized by its maximum at 440 nm, corresponding to a system of extensively conjugated π-electrons that declined during the reaction time. It is probably attributed to breaking the single bonds of-CH= or -N= groups that destroy the conjugated system.

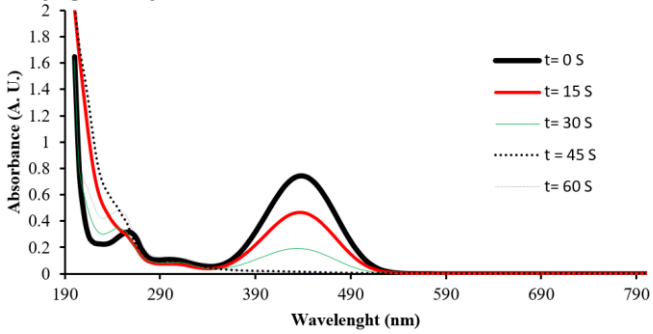

Figure 4. The variation of UV-Vis spectra during the decolorization of BY 28 in sonoelectrochemical process in the optimized condition: Conditions: BY 28 solution volume: 600 mL; [BY 28]: 0.076 mmolL^{-1}; electric voltage:11.15V; ultrasonic power : 529.7 W; pH : 5.0; temperature= 21.8˚C and [KCl]: 0.08 molL^{-1}.

3. 9. HPLC-UV analysis

The decolorization of BY 28 and the appearance of degradation products were also investigated by high-pressure liquid chromatography (HPLC) analysis. Samples were taken from the reaction vessels and filtered through 0.45 µm cellulose membranes (Millex, Millipore). After treatment, the residuals were determined by HPLC-UV, which was set to 254 nm. The sample loop volume was 20 µL, and the mobile-phase composition was a mixture of (55:45 V/V) acetonitrile:water with a flow rate of 1 mLmin^{-1}. A 25 µL LC microsyringe (ILS, stutzerbach, Germany) was used for sample injection. The HPLC elution profiles of BY 28 before and after sonoelectrochemical treatment is depicted in Fig.5. As it is shown, the intense chromatogram at 2.6 min that is related to BY 28 disappears for the treated sample, and instead, three new chromatogram with significant shorter retention times (1.18, 1.23, 1.42 min; Fig. 5) are developed. These diminished times suggest forming more polar derivatives than the primary substance.

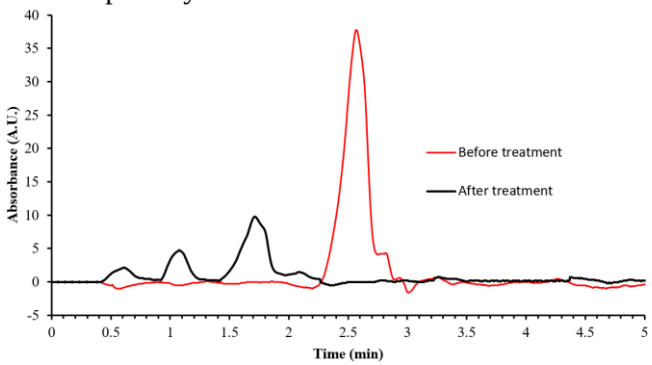

Figure 5. HPLC chromatograms before and after of the sonoelectrochemical treatment. Conditions: BY 28 solution volume: 600 mL; [BY 28]: 0.076 mmolL^{-1}; electric voltage:11.15 V; ultrasonic power:529.7 W; pH: 5.0; temperature= 21.8 ˚C and [KCl]: 0.08 molL^{-1}.

3. 10. GC-MS analysis

An aqueous solution of BY 28 (50 ppm) was treated for 1 min according to the proposed degradation process to identify intermediate products. After decolorization, the solution was extracted twice with CH_2Cl_2 using a separating funnel and dried to remove the remaining moisture using $CaCl_2$ for GC-MS analysis. Different degradation products identified at different elution times are given in Table 4 with their mass/charge (m/z) ratio. From the identified straight chain intermediate products like anisole, N-Methyl-p-anisidine, trimethylindolenine, and small amounts of phenol, it is evident that BY 28 has been extensively degraded after 1 min.

3.11. Comparison with other methods

The characteristics of the developed method for the decolorization of BY 28 were compared to some of the previously reported electrochemically methods (Table 5). Based on the results, the proposed method with a relatively large sample volume, resistant and relatively

cheap electrodes, and very short treatment time has some remarkable advantages compared to the previous reports.

Table 4. Identification of main degradation intermediates by GC-MS after 1 min sonoelectrochemical treatment of BY28.

No.	Retention time (min)	Peak area (%)	m/z	Intermediate product
1	3.241	24.09	137.08	N-Methyl-p-anisidine
2	3.680	22.74	108.06	Anisole
3	3.912	1.12	94.04	Phenol
4	5.835	16.18	164.09	-
5	6.256	35.87	161.25	Trimethylindolenine

Table 5. Comparison of the method with the other reported for BY 28

Decolorization method	Type of electrode		Time	Decolorization	Conc.	Volume	
	Cathode	Anode	(min)	(%)	(mgL^{-1})	(mL)	Ref.
Electrocoagulation	Iron(ST 37-2)	Iron(ST 37-2)	7	~ 95%	50	250	[14]
Indirect electrochemistry	Iron(SS 304)	Ti/PtOx	60	~ 95%	70	500	[15]
Electrochemical/ biological oxidation	Pt	Pb/PbO_2	180	~100%	134	500	[16]
Photoelectro-fenton	CNT–PTFE[a]	Pt	360	94.7	20	2000	[11]
Electrochemistry	Co-PVC[b]	Co-PVC	60	98	80	50	[17]
Sonoelectrochemistry	Iron(SS 316)	Iron(SS 316)	1	99.7%	33	600	This work

[a] Carbon nanotube–polytetrafluoroethylene, [b]Co-polyvinylchloride.

4. Conclusion

The developed sonoelectrochemical process was an effective method for treating colored wastewater. Using persistent and cheap electrodes, a relatively large volume of BY 28 solution was almost wholly decolorized according to the present method. As a preliminary step, effective factors and their experimental ranges were determined. Optimization of the categorical factors was conducted using the OFAT method. In contrast, a half-fractional CCD was used for the numerical factors, and two different mathematical equations were obtained for the decolorization percentage and energy efficiency.

Furthermore, the desirability function was used to resolve the multi-response problem and get a maximum decolorization with minimum electrical energy consumption. Under the optimized conditions, the decolorization% of 97.5±1.1% and energy efficiency of 0.75±0.06mmol kWh^{-1}, which was achieved that was close to predicted values. This method was tested as a pilot treatment plant, which makes it viable for larger scales. A comparison of the developed method confirmed that it is more efficient than the other previous methods.

References

[1] G. K. G. Carvalho Barros, L. J. N. Duarte, R. P. F. Melo, F. W. B. Lopes, & E. L. Barros Neto, Ionic Dye Removal Using Solvent-Assisted Ionic Micellar Flocculation, *Journal of Polymers and the Environment*, 30 (2022) 2534-2546.

[2] M. Zabihi, & A. Motavalizadehkakhky, PbS/ZIF-67 nanocomposite: novel material for photocatalytic degradation of basic yellow 28 and direct blue 199 dyes, *Journal of the Taiwan Institute of Chemical Engineers*, 140 (2022) 104572.

[3] T. B. Budak, The investigation of basic yellow 28 adsorption by using different carbon material, *The European Journal of Research and Development*, 2 (2022) 106-114.

[4] T. A. Aragaw, & A. N. Alene, A comparative study of acidic, basic, and reactive dyes adsorption from aqueous solution onto kaolin adsorbent: Effect of operating parameters, isotherms, kinetics, and thermodynamics, *Emerging Contaminants*, 8 (2022) 59-74.

[5] E. Kohan, & A. Shiralizadeh Dezfuli, Environmentally friendly decolorization of textile dye CI yellow 28 in water by Bi2− x (Lu, Er) xO3 nanoparticles, *Journal of Materials Science: Materials in Electronics*, 30 (2019) 17170-17180.

[6] S. Benkaddour, I. El Ouahabi, H. Hiyane, M. Essoufy, A. Driouich, S. El Antri, ... & S. Lazar, Removal of Basic Yellow 28 by biosorption onto watermelon seeds, part I: The principal factors influencing by Plackett-Burman screening design, *Surfaces and Interfaces*, 21 (2020) 100732.

[7] N. Tekin, A. Şafaklı, D. Bingöl, Process modeling and thermodynamics and kinetics evaluation of Basic Yellow 28 adsorption onto sepiolite, *Desalination and Water Treatment*, 54 (2015) 2023-2035.

[8] N. Dahdouh, S. Amokrane, R. Murillo, E. Mekatel, & D. Nibou, Removal of methylene blue and basic yellow 28 dyes from aqueous solutions using sulphonated waste poly methyl methacrylate, *Journal of Polymers and the Environment*, 28 (2020) 271-283.

[9] M. Zabihi, & A. Motavalizadehkakhky, PbS/ZIF-67 nanocomposite: novel material for photocatalytic degradation of basic yellow 28 and direct blue 199 dyes,

Journal of the Taiwan Institute of Chemical Engineers, 140 (2022) 104572.
[10] H. Niknam, & A. Sadeghzadeh-Attar, Mg-doped TiO2 nanorods-SrTiO3 heterojunction composites for efficient visible-light photocatalytic degradation of basic yellow 28, *Optical Materials*, 136 (2023) 113395.
[11] M. Iranifam, M. Zarei, A. Khataee, Decolorization of CI Basic Yellow 28 solution using supported ZnO nanoparticles coupled with photoelectro-Fenton process, *Journal of electroanalytical chemistry*, 659 (2011) 107-112.
[12] T. Poursaberi, M. Hassanisadi, & F. Nourmohammadian, Application of synthesized nanoscale zero-valent iron in the treatment of dye solution containing basic yellow 28, (2012).
[13] R.M. Belal, M.A. Zayed, R.M. El-Sherif, & N. A.A. Ghany, Advanced electrochemical degradation of basic yellow 28 textile dye using IrO_2/Ti meshed electrode in different supporting electrolytes. *Journal of Electroanalytical Chemistry*, 882 (2021) 114979.
[14] A. Akbarpour, A. Khataee, M. Fathinia, & B. Vahid, Development of kinetic models for photoassisted electrochemical process using Ti/RuO2 anode and carbon nanotube-based O2-diffusion cathode, *Electrochimica Acta*, 187 (2016) 300-311.
[15] I. Yahiaoui, F. Aissani-Benissad, F. Fourcade, & A. Amrane, Enhancement of the biodegradability of a mixture of dyes (methylene blue and basic yellow 28) using the electrochemical process on a glassy carbon electrode, *Desalination and Water Treatment*, 57 (2016) 12316-12323.
[16] I. Yahiaoui, F. Aissani- Benissad, F. Fourcade, A. Amrane, Combination of an electrochemical pretreatment with a biological oxidation for the mineralization of nonbiodegradable organic dyes: basic yellow 28 dye, *Environmental Progress & Sustainable Energy*, 33 (2014) 160-169.
[17] P. V. Nidheesh, M. Zhou, & M. A. Oturan, An overview on the removal of synthetic dyes from water by electrochemical advanced oxidation processes, *Chemosphere*, 197 (2018) 210-227.
[18] E. Brillas, C.A. Martínez-Huitle, Decontamination of wastewaters containing synthetic organic dyes by electrochemical methods. An updated review, A*pplied Catalysis B: Environmental*, 166 (2015) 603-643.
[19] V. K. Gupta, S. Khamparia, I. Tyagi, D. Jaspal, & A. Malviya, Decolorization of mixture of dyes: A critical review, (2015).
[20] D. K. Sarfo, A. Kaur, D. L. Marshall, & A. P. O'Mullane, Electrochemical degradation and mineralisation of organic dyes in aqueous nitrate solutions, *Chemosphere*, (2023) 137821.
[21] R. M. Belal, M. A. Zayed, R. M. El-Sherif, & N. A. A. Ghany, Electrochemical Degradation and Degree of Mineralization of the BY28 Dye in a Supporting Electrolyte Mixture Using an Expanded Dimensionally Stable Anode, *Electrocatalysis*, 13 (2022) 26-36.
[22] I. Naser, D. Safarvand, M. Samipour Gir, & M. Ardjmand, Electrochemical degradation of Basic Yellow dye using a Ce@ PbO2 anode: Optimization of operational parameters. Iranian (Iranica) *Journal of Energy & Environment*, (2022) (Articles in Press).
[23] P. Treegosol, J. Priyadumkol, W. Kamutavanich, K. Katchasuwanmanee, & W. Chaiworapuek, Experimental investigation of the heat transfer and friction loss of turbulent flow in circular pipe under low-frequency ultrasound propagation along the mainstream flow, *Ultrasonics*, 128 (2023) 106866.
[24] W. Hoeben, E. Van Veldhuizen, W. Rutgers, G. Kroesen, Gas phase corona discharges for oxidation of phenol in an aqueous solution, J*ournal of Physics D: Applied Physics*, 32 (1999) L133.
[25] R. Mohammadi, M.A. Mohammadifar, A.M. Mortazavian, M. Rouhi, J.B. Ghasemi, Z. Delshadian, Extraction optimization of pepsin-soluble collagen from eggshell membrane by response surface methodology (RSM), *Food chemistry*, 190 (2016) 186-193.
[26] A. Al- Zuheri, H. S. Ketan, & I. Vlachos, Grouping technology and a hybrid genetic algorithm- desirability function approach for optimum design of cellular manufacturing systems, *IET Collaborative Intelligent Manufacturing*, (2022).
[27] M. A. Bezerra, S. L. C. Ferreira, C. G. Novaes, A. M. P. Dos Santos, G. S. Valasques, U. M. F. da Mata Cerqueira, & J. P. dos Santos Alves, Simultaneous optimization of multiple responses and its application in Analytical Chemistry–A review, *Talanta*,194 (2019) 941-959.
[28] N. Chamkouri, A. Niazi, V. Zare-Shahabadi, Development of a novel pH sensor based upon Janus Green B immobilized on triacetyl cellulose membrane: Experimental design and optimization, *Spectrochimica Acta Part A: Molecular and Biomolecular Spectroscopy*, 156 (2016) 105-111.